Author(s): Dahlous, Kholood A.; Soliman, Saied M.; Haukka, Matti; El-Faham, Ayman; Massoud, Raghdaa A.

Title: A New 1D Ni (II) Coordination Polymer of s-Triazine Type Ligand and Thiocyanate as Linker via Unexpected Hydrolysis of 2,4-Bis(3,5-dimethyl-1H-pyrazol-1-yl)-6-methoxy-1,3,5-triazine

Year: 2023

Version: Published version

Please cite the original version:

Dahlous, K. A., Soliman, S. M., Haukka, M., El-Faham, A., & Massoud, R. A. (2023). A New 1D Ni (II) Coordination Polymer of s-Triazine Type Ligand and Thiocyanate as Linker via Unexpected Hydrolysis of 2,4-Bis(3,5-dimethyl-1H-pyrazol-1-yl)-6-methoxy-1,3,5-triazine. Inorganics, 11(3), Article 135. https://doi.org/10.3390/inorganics11030135

inorganics

MDPI

Article

A New 1D Ni (II) Coordination Polymer of *s*-Triazine Type Ligand and Thiocyanate as Linker via Unexpected Hydrolysis of 2,4-*Bis*(3,5-dimethyl-1*H*-pyrazol-1-yl)-6-methoxy-1,3,5-triazine

Kholood A. Dahlous [1,*], Saied M. Soliman [2,*], Matti Haukka [3], Ayman El-Faham [2] and Raghdaa A. Massoud [2]

[1] Department of Chemistry, College of Science, King Saud University, P.O. Box 2455, Riyadh 11451, Saudi Arabia
[2] Department of Chemistry, Faculty of Science, Alexandria University, P.O. Box 426, Ibrahimia, Alexandria 21321, Egypt; aymanel_faham@hotmail.com (A.E.-F.); raghdaamassoud@yahoo.com (R.A.M.)
[3] Department of Chemistry, University of Jyväskylä, P.O. Box 35, FI-40014 Jyväskylä, Finland; matti.o.haukka@jyu.fi
* Correspondence: kdahloos@ksu.edu.sa (K.A.D.); saied1soliman@yahoo.com (S.M.S.); Tel.: +20-111-136-1059 (S.M.S.)

Abstract: A new 1D Ni(II) coordination polymer was synthesized by the reaction of $NiSO_4 \cdot 6H_2O$ with 2,4-*bis*(3,5-dimethyl-1*H*-pyrazol-1-yl)-6-methoxy-1,3,5-triazine (BPT) and SCN^- as a linker in an acidic medium by heating under reflux conditions. Unusually, the BPT ligand underwent acid-mediated hydrolysis by losing one of the pyrazolyl arms afforded the polymeric $[Ni(MPT)(H_2O)(SCN)_2]_n$ complex (MPT: 4-(3,5-dimethyl-1*H*-pyrazol-1-yl)-6-methoxy-1,3,5-triazin-2-ol. The Ni(II) center is coordinated with one MPT as a bidentate *NN*-chelate, one water molecule, and two thiocyanate groups in *cis* positions to one another. One of the thiocyanate groups acts as a bridging ligand between metal centers, leading to a one-dimensional polymeric structure that extends along the *c*-direction. The other thiocyanate group is terminally N-coordinated. The $[Ni(MPT)(H_2O)(SCN)_2]_n$ complex has been screened in vitro against two pathogenic fungal strains: *A. fumigatus*, *C. albican*, and four pathogenic bacterial strains: *S. aureus*, *B. subtilis* as gram-positive bacteria, *E. coli*, *P. vulgaris* as gram-negative bacteria. The results showed that the complex has the potential to be used as both an antibacterial and an antifungal agent. Also, the $[Ni(MPT)(H_2O)(SCN)_2]_n$ complex showed cytotoxic activities against hepatocellular (HepG-2) and lung (A-549) cell lines, with IC_{50} values of 132.67 ± 5.14 and 146.97 ± 7.34 µM, respectively.

Keywords: nickel (II); s-triazine; antimicrobial; cytotoxicity; liver and lung carcinomas

Citation: Dahlous, K.A.; Soliman, S.M.; Haukka, M.; El-Faham, A.; Massoud, R.A. A New 1D Ni (II) Coordination Polymer of *s*-Triazine Type Ligand and Thiocyanate as Linker via Unexpected Hydrolysis of 2,4-*Bis*(3,5-dimethyl-1*H*-pyrazol-1-yl)-6-methoxy-1,3,5-triazine. *Inorganics* **2023**, *11*, 135. https://doi.org/10.3390/inorganics11030135

Academic Editor: Vladimir Arion

Received: 7 March 2023
Revised: 15 March 2023
Accepted: 17 March 2023
Published: 22 March 2023

1. Introduction

In the literature, multi-functional chelating ligands sparked the interest of scientists due to their remarkable applications in different areas. Of polydentate ligands, the highly symmetric *s*-triazine scaffold with heterocyclic groups attached to it is important for a wide range of applications in pharmaceutical chemistry [1] due to their widespread antimicrobial [2], anticancer [3,4], and antiviral activities [5]. Especially, *s*-triazine compounds bearing a pyrazole moiety were found to have low toxicity toward growth-stimulating activity [6,7]. Many of their derivatives showed moderate-to-strong anticancer activities, which were found to depend on the type of groups attached to the *s*-triazine core [8]. *s*-Triazines are also employed in diverse industries such as plastic [9], electrical [10], dye [11], production of ion-exchange resins and cleaning wastewater [12], pesticides [13], optical switches [14,15], low-toxicity flame-retardant materials [16], and as a replacement for some raw materials in petrochemical industries [17]. Also, these nitrogen-rich molecules have potential use as energetic explosives [18] and organic corrosion inhibitors [19]. This class of versatile chelating agents has a weak ligand field [20] and is characterized by the presence

of the symmetric triazine core, which is an essential feature in crystal engineering [21,22] and an important factor in building stable high-spin metal complexes [23] with extended molecular and supramolecular architectures [24,25], which are widely used in various magnetic [26] and catalytic applications [27,28].

In our previous work with *s*-triazine pincer ligands comprising two pyrazolyl arms, we reported the molecular and supramolecular structures of different metal pincer complexes with a *bis*-pyrazolyl-*s*-triazine ligand [3,6,20,23–25,29–42]. Many homoleptic and heteroleptic complexes of this type with pincer ligands and divalent and trivalent metal ions were reported to have coordination numbers ranging from five to eight. 2,4-*Bis*(3,5-dimethyl-1*H*-pyrazol-1-yl)-6-methoxy-1,3,5-triazine is an interesting N-pincer ligand that continues to receive the interest of our research group (BPT; Figure 1) and was used for the synthesis of a large number of polymeric and discrete metal (II) complexes [29–42]. It is noted that the coordination behavior of the pincer *bis*-pyrazolyl-*s*-triazine ligand (BPT) depends on many factors, such as the type of metal ion, reaction conditions such as medium and temperature, as well as the nature of the counter anion. In the majority of cases, the discrete pincer complexes of the *bis*-pyrazolyl-*s*-triazine ligand were obtained [3,6,20,23–25,29,30,34–38,41,42]. In some instances, the ligand underwent hydrolysis, either catalyzed by the medium acidity of an external acid [31] or by the Lewis acidity of the metal ion [23,31–33]. In this regard, the methoxy group of the BPT ligand underwent hydrolysis in the presence of $Cu(ClO_4)_2{\cdot}6H_2O$ or $FeCl_3$, while the hydrolysis was continued at one of the pyrazolyl moieties in the presence of $CuCl_2$ or $PdCl_2$. Figure 1 shows the structures of the hydrolyzed ligands HL_1 and HL_2, respectively. In the case of the two Cu(II) salts, the 1D coordination polymers $[Cu_2(L_1)(ClO_4)_3(H_2O)_4]{\cdot}2H_2O$ and $[Cu(L_2)(H_2O)Cl]$ of the hydrolyzed ligands were obtained as final products. These *s*-triazine ligands are found coordinated with the Cu(II) ion as mononegative bidentate chelates. In the case of $FeCl_3$, the hydrolysis of BPT afforded the mononuclear $[Fe(L_1)(CH_3OH)Cl_2]$ pincer complex, and the hydrolyzed ligand (HL_1) is found coordinated to Fe(III) as a mononegative tridentate pincer chelate. For $PdCl_2$, the hydrolyzed *s*-triazine ligand (HL_2) also as a mononegative bidentate chelate, but the corresponding mononuclear Pd(II) complex $[Pd(L_2)(H_2O)Cl]$ was formed in this case. In the presence of HCl (1:1 *v*/*v*) in an aqueous solution, the hydrolysis of BPT was found to depend on the reaction conditions. The hydrolysis reaction occurred for the methoxy group and one of the two pyrazolyl moieties by stirring the BPT ligand with HCl at room temperature for 2–3 h, and the final product was the free HL_2. In the presence of more vigorous conditions of heating under reflux, the complete hydrolysis of BPT occurred, and the final product was approved as 1,3,5-triazine-2,4,6-triol. Interestingly, the reaction of BPT with $Fe(NO_3)_3$ also proceeded with the hydrolysis to HL_1, and the final product was the μ-oxo diiron complex of the formula $[Fe_2(L_1)_2(H_2O)_4O](NO_3)_2$ [43].

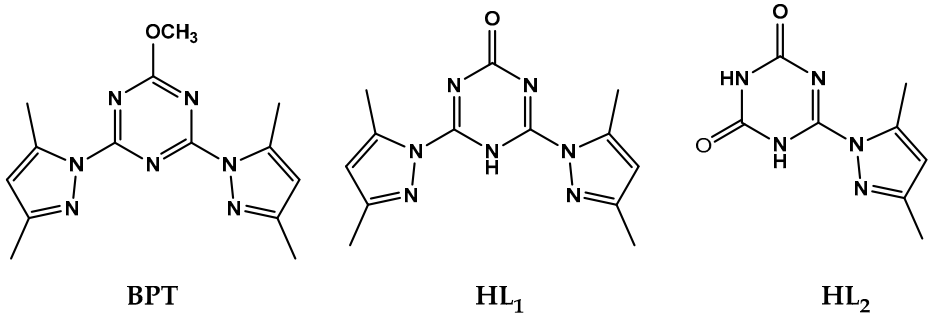

Figure 1. Structure of the studied ligand (BPT) and its hydrolyzed ligands HL_1 and HL_2.

Metal ions play an important role in the cell's life and in biology. Of these metal ions, nickel has a significant biological role in the active center of the urease enzyme [44] and others [45,46]. Moreover, a great number of nickel complexes having interesting biological activity have been reported for their antifungal [47], anti-inflammatory [48], and antioxidant [49,50] activities. Some Ni (II) complexes bearing N,O-chelating ligands are active

towards polymerization, and the resulting coordination polymers were found to have interesting applications in catalysis [51] and biology [52]. In addition, they showed prospective applications as luminescent [53], conductive [54], and for the recovery of trace metal ions [55]. Dong and coworkers reported the structure and magnetic properties of some Ni(II) coordination polymers based on 2,4-[6-(4-carboxyphenyl)pyrazin-2-yl]benzoic acid as a NO-donor ligand [56]. The last decade has witnessed an upsurge in research efforts for the development of coordination polymers, which have interesting molecular architectures due to their novel and diversified structural characteristics. In this regard, polymeric coordination compounds based on *s*-triazine have interesting magnetic properties and great industrial importance [57–59].

As a continuation of our recent work concerning metal-*s*-triazine complexes with pseudohalides as auxiliary ligands [39,40], our current research is focused on the synthesis of a new polymeric Ni(II) complex with a *s*-triazine-type ligand employing SCN^- as an auxiliary bridging ligand. The reaction was performed by mixing $NiSO_4.6H_2O$, the BPT ligand, and SCN^- in the presence of diluted sulfuric acid to increase the possibility of the hydrolysis of the BPT ligand, which in turn increases the possibility of obtaining the coordination polymer rather than the discrete complex. The structural aspects of the synthesized complex were analyzed using single-crystal X-ray diffraction and FTIR spectroscopy. To evaluate the biological impact of the new Ni(II) complex, the cytotoxicity against some cancer cell lines in addition to the antimicrobial activity were reported.

2. Results and Discussion

2.1. Synthesis and Characterizations

It was reported that the reactions of the BPT ligand with Ni(II) salts comprising different anions (NO_3^-, Cl^-, and ClO_4^-) have afforded a variety of mononuclear Ni(II)-BPT complexes (Scheme 1) [41,42]. The same ligand (BPT) underwent hydrolysis in the presence of metal ions, leading to polymeric metal-organic frameworks [31]. Also, similar hydrolytic reactions were detected in the presence of acid. It was found that the methoxy group is the most prominent group for hydrolysis at first, followed by either one or both of the pyrazolyl moieties. In continuation of the work on this N-pincer ligand, we presented here the reaction of the *s*-triazine functional ligand (BPT) with nickel sulfate hexahydrate in the presence of SCN^- as a co-ligand in an acidic medium by heating under reflux. The target of the addition of KSCN solution during the reaction is to construct a Ni(II)-thiocyanato coordination polymer comprising the *s*-triazine ligand. As expected, the BPT ligand underwent acid-mediated hydrolysis, but in this case a cleavage of one of the C-N bonds between the pyrazole and *s*-triazine moieties occurred, leading to the formation of 4-(3,5-dimethyl-1*H*-pyrazol-1-yl)-6-methoxy-1,3,5-triazin-2-ol (MPT), which in situ reacts with Ni(II) and affords the new $[Ni(MPT)(H_2O)(SCN)_2]_n$ complex as a final product in a good yield (76.4%). Its structure was confirmed by elemental analysis and FTIR spectra, and the polymeric framework was unambiguously confirmed by single-crystal X-ray diffraction. The antimicrobial activity of the new $[Ni(MPT)(H_2O)(SCN)_2]_n$ complex was evaluated against two pathogenic fungal strains: Aspergillus fumigatus and Candida albicans, and four pathogenic bacterial strains: Staphylococcus aureus, Bacillus subtilis as gram-positive bacteria, Escherichia coli, and Proteus vulgaris as gram-negative bacteria, as reported here. The obtained results were compared with Ketoconazole and Gentamycin as positive antifungal and antibacterial controls, respectively. In addition, the anticancer activity of the $[Ni(MPT)(H_2O)(SCN)_2]_n$ complex was examined against hepatocellular (HepG-2) and lung (A-549) carcinomas, and the results were compared with *cis*-platin as a positive control. The $[Ni(MPT)(H_2O)(SCN)_2]_n$ complex is freely soluble in DMSO, DMF, ethanol, and methanol. In contrast, this complex is insoluble in water, carbon tetrachloride, and cyclohexane.

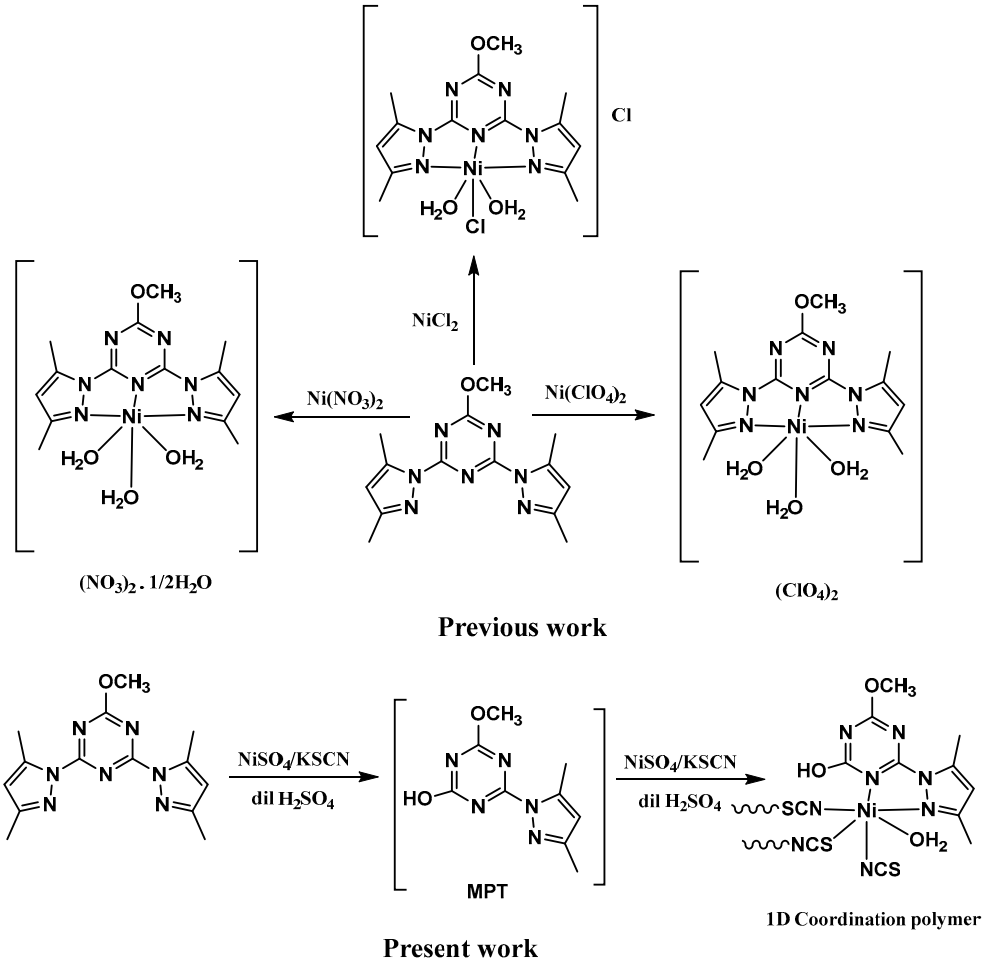

Scheme 1. Synthesis of the previously reported Ni(II)-BPT complexes (**upper**) and the current Ni(II) coordination polymer (**lower**).

2.2. Crystal Structure Description

The structure of the $[Ni(MPT)(H_2O)(SCN)_2]_n$ complex is shown in Figure 2, while the crystallographic details are listed in Table 1, and the selected geometric parameters (bond distances and angles) are presented in Table 2. The polymeric $[Ni(MPT)(H_2O)(SCN)_2]_n$ complex is found crystallized in the monoclinic crystal system and the $P2_1/c$ space group. The unit cell parameters are a = 16.0718(5) Å, b = 11.0571(4) Å, c = 10.6401(4) Å, and β = 90.889(2)°, while the unit cell volume is 1890.60(11) Å^3. The asymmetric unit comprised one $[Ni(MPT)(H_2O)(SCN)_2]$ formula unit. As clearly seen from Figure 2, the coordination sphere of this neutral complex contains one MPT ligand, one water molecule, and two differently coordinated thiocyanate groups.

In this complex, the Ni(II) is hexa-coordinated with a NiN_4SO coordination sphere. The organic ligand (MPT) acts as a bidentate chelate via the nitrogen atom from the pyrazole moiety [Ni1-N1; 2.074(3) Å] and one of the s-triazine nitrogen atoms [Ni1-N5; 2.080(3) Å]. The bite angle of this ligand is 77.46(10)°. In addition, Ni(II) is coordinated to one water molecule [Ni1-O3; 2.086(3) Å], which is found trans to the Ni1-N1 bond of the pyrazole moiety. The coordination sphere of the Ni(II) in the asymmetric unit is completed by two interactions with two SCN^- groups in cis-positions to one another, forming the equatorial plane of the NiN_4SO octahedron with Ni1-N6 and Ni1-N7 distances of 2.033(3) Å and 2.053(4) Å, respectively. It is worth noting that one of the two thiocyanate groups is acting as a terminal N-donor ligand, while the other thiocyanate group is bridging between the Ni(II) centers. This bridging thiocyanate group connects the $[Ni(MPT)(H_2O)(NCS)_2]$ complex unit with another one via the long Ni1-S2$^{\#}$ distance of 2.5755(10) Å. Hence, the

supramolecular structure of the complex $[Ni(MPT)(H_2O)(SCN)_2]_n$ could be described as a one-dimensional zigzag-like coordination polymer of the complex units connected by the bridged thiocyanate group through the crystallographic c-direction as shown in Figure 3. The angles between the trans bonds in the equatorial positions are in the range of 174.56(12)° for N6-Ni1-N5 to 176.59(10)° for N7-Ni1-S2$^{\#}$ angles, while the bond angle of axial trans bonds is in turn equal to 170.73(10) ° for N1-Ni1-O3 angle. Additionally, the angles between the cis-bonds are to a great extent close to the ideal case of the perfect octahedron, where N6-Ni1-N7, N6-Ni1-N1, and N7-Ni1-N1 angles are 91.93(13), 99.10(11) and 91.17(13)°, respectively (Table 2). As a result, the complex has a slightly distorted octahedral coordination environment.

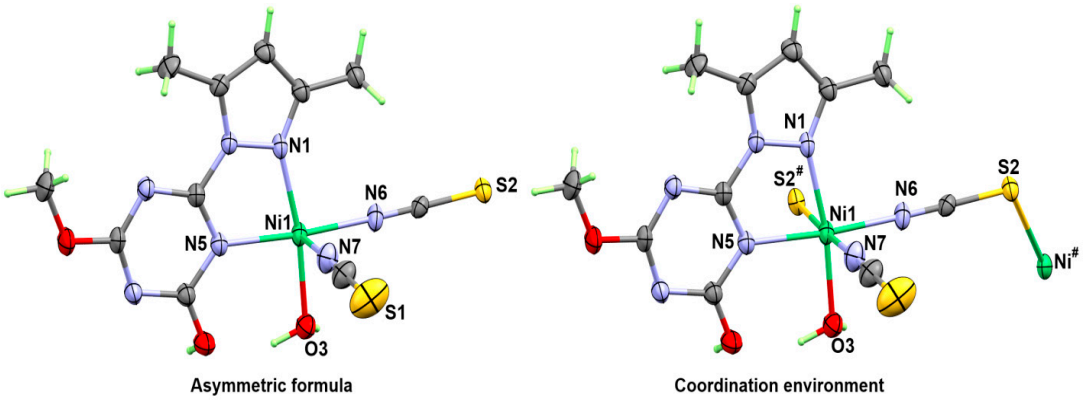

Figure 2. The X-ray structure of the $[Ni(MPT)(H_2O)(SCN)_2]_n$ complex. Symmetry code #: x,1.5 − y,1/2 + z.

Table 1. Crystallographic data for the $[Ni(MPT)(H_2O)(SCN)_2]_n$ complex.

	$[Ni(MPT)(H_2O)(SCN)_2]_n$
CCDC	2231954
empirical formula	$C_{11}H_{13}N_7NiO_3S_2$
fw	414.11
temp (K)	289(2) K
λ (Å)	0.71073
cryst syst	Monoclinic
space group	$P2_1/c$
a (Å)	16.0718(5)
b (Å)	11.0571(4)
c (Å)	10.6401(4)
β (deg)	90.889(2)
V (Å^3)	1890.60(11)
Z	4
ρ_{calc} (Mg/m^3)	1.455
μ (Mo Kα) (mm^{-1})	1.270
No. reflns.	22,147
Unique reflns.	4684
Completeness to θ = 25.242°	99.9
GOOF (F^2)	1.050
R_{int}	0.0538
R_1 [a] ($I \geq 2\sigma$)	0.0493
wR_2 [b] ($I \geq 2\sigma$)	0.1114

[a] $R_1 = \sum ||F_o| - |F_c|| / \sum |F_o|$. [b] $wR_2 = \{\sum [w(F_o^2 - F_c^2)^2] / \sum [w(F_o^2)^2]\}^{1/2}$.

Table 2. The most important bond distances and angles in the [Ni (MPT)(H_2O)($SCN)_2$]$_n$ complex.

Bond	**Distance**	**Bond**	**Distance**
Ni (1)-N (6)	2.033(3)	Ni (1)-N (5)	2.080(3)
Ni (1)-N (7)	2.053(4)	Ni (1)-O (3)	2.086(3)
Ni (1)-N (1)	2.074(3)	Ni (1)-S (2) #1	2.5755(10)
Bonds	**Angle**	**Bonds**	**Angle**
N(6)-Ni(1)-N(7)	91.93(13)	N(1)-Ni(1)-O(3)	170.73(10)
N(6)-Ni(1)-N(1)	99.10(11)	N(5)-Ni(1)-O(3)	93.29(11)
N(7)-Ni(1)-N(1)	91.17(13)	N(6)-Ni(1)-S(2)#1	84.66(9)
N(6)-Ni(1)-N(5)	174.56(12)	N(7)-Ni(1)-S(2)#1	176.59(10)
N(7)-Ni(1)-N(5)	92.34(12)	N(1)-Ni(1)-S(2)#1	89.21(8)
N(1)-Ni(1)-N(5)	77.46(10)	N(5)-Ni(1)-S(2)#1	91.05(8)
N(6)-Ni(1)-O(3)	90.09(12)	O(3)-Ni(1)-S(2)#1	90.41(8)
N(7)-Ni(1)-O(3)	89.76(13)	C(11)-S(2)-Ni(1)#2	107.68(12)
Ni(1)#2-S(2)-N(1)#2	39.16(5)	Ni(1)-O(3)-H(3A)	109.7
Ni(1)-O(3)-H(3B)	109.9	C(1)-N(1)-Ni(1)	141.2(2)
N(2)-N(1)-Ni(1)	112.8(2)	C(6)-N(5)-Ni(1)	116.2(2)
C(9)-N(5)-Ni(1)	128.4(2)	C(11)-N(6)-Ni(1)	172.0(3)
C(10)-N(7)-Ni(1)	175.9(4)		

Symme. codes: #1 x,−y + 3/2,z − 1/2 #2 x, −y + 3/2,z + 1/2.

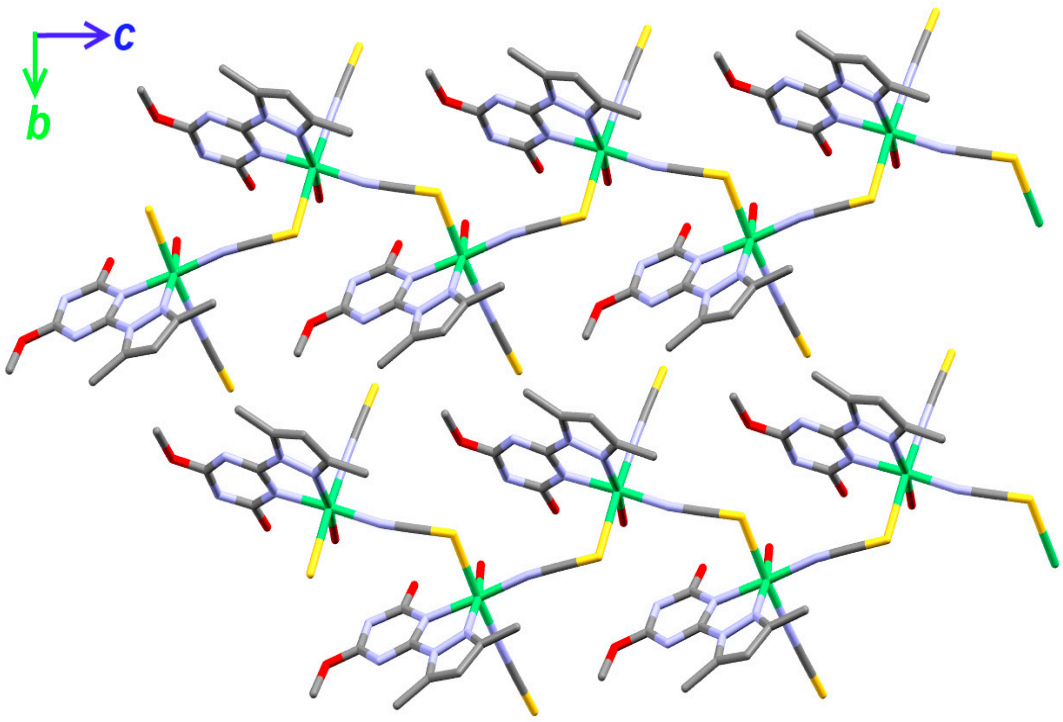

Figure 3. The packing scheme of the 1D polymeric structure of the [Ni(MPT)(H_2O)($SCN)_2$]$_n$ complex. All H-atoms were omitted for better clarity.

The supramolecular structure of the [Ni(MPT)(H_2O)($SCN)_2$]$_n$ complex showed some weak O-H . . . C and C-H . . . S non-covalent interactions that connect the 1D polymer chains together. The O3-H3B . . . C9 interaction occurs between one of the O-H bonds from the coordinated water molecule and the C9 atom from the s-triazine moiety. The donor (O3) to acceptor (C9) interaction distance is determined to be 3.388(4) Å. In addition, the C5-H5B from one of the methyl groups forms a relatively short interaction with the S2 atom from the bridged thiocyanate group. The donor (C5) to acceptor (S2) interaction distance is determined to be 3.013 Å. Views of the 1D polymer chains connected by the C5-H5B . . . S2 and O3-H3B . . . C9 interactions are shown in Figures 4A and 4B, respectively.

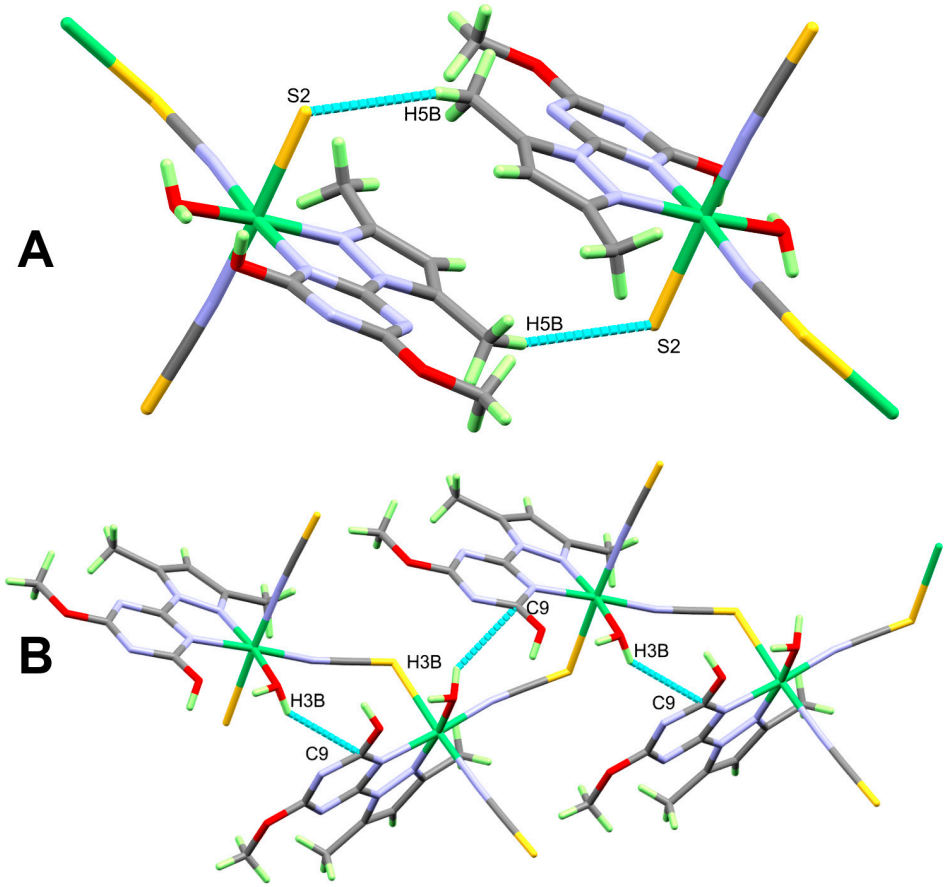

Figure 4. The C-H . . . S (**A**) and O-H . . . C (**B**) interactions connecting the 1D polymer backbone of the $[Ni(MPT)(H_2O)(SCN)_2]_n$ complex.

2.3. FTIR Spectra

The FTIR spectra of the $[Ni(MPT)(H_2O)(SCN)_2]_n$ complex are shown in Figure S1 (Supplementary Materials). The results revealed the presence of the main vibrational fundamentals of the $[Ni(MPT)(H_2O)(SCN)_2]_n$ complex. For the BPT ligand, the FTIR spectra showed the ν(C=N) and ν(C=C) vibrational characteristics at 1593 cm^{-1} and 1555 cm^{-1}, respectively [60,61]. The bands appeared at 3041 and 2978–2926 cm^{-1} were assigned for the aromatic and aliphatic ν(C-H) modes. The respective values for the $[Ni(MPT)(H_2O)(SCN)_2]_n$ complex were detected at 2991 and 2929 cm^{-1}, respectively. Also, the broad band detected at 3416 cm^{-1} could be assigned to the ν(O-H) modes in the complex. The ν(C=N) and ν(C=C) vibrational characteristics in the Ni(II) complex were detected at higher wavenumbers of 1603 and 1565 cm^{-1}, respectively. Also, an intense sharp peak was detected at 2114 cm^{-1}, corresponding to the stretching vibrations of the thiocyanate group. This sharp peak represents the CN stretching frequencies of the two NCS groups found in the $[Ni(MPT)(H_2O)(SCN)_2]_n$ complex.

2.4. Biological Studies

2.4.1. Antimicrobial Activity

The antimicrobial activity of the $[Ni(MPT)(H_2O)(SCN)_2]_n$ complex was performed using the well diffusion agar technique against two pathogenic fungal strains: *A. fumigatus*, *C. albican*, and four pathogenic bacterial strains: *S. aureus*, *B. subtilis* as gram-positive bacteria, *E. coli*, and *P. vulgaris* as gram-negative bacteria. Results of the initial assessment of the Ni(II) complex as an antimicrobial agent against these selected harmful organisms are presented in Table 3. This table shows the diameter of different inhibition zones resulting from the treatment of these microbes by the studied complex, which in turn indicates the

bioactivity of the prepared complex against these microbes. The activities of the complex were also compared with those of ketoconazole and gentamycin, which were used as antifungal and antibacterial positive controls, respectively. The inhibition zone diameters were found to be in the range of 12–18 mm at 10 mg/mL of the investigated compound. The presented Ni(II) complex has significant anti-fungal activity since the inhibition zone diameter for *A. fumigatus* was found to be 14 mm, which is close to that of the antifungal control ketoconazole (18 mm). Also, the tested Ni(II) complex exhibited a higher tendency to inhibit the growth of the fungus *A. fumigatus* (14 mm) than *C. albican* (12 mm). In terms of antibacterial activity, the Ni(II) complex has good actions against the tested bacteria to different extents. The inhibition zone diameters are 16 and 18 mm for *S. aureus* and *B. subtilis* as gram-positive bacteria, respectively. For Gentamycin, the respective values of the inhibition zone diameters are 24 and 26 mm. In the case of *E. coli* and *P. vulgaris* as gram-negative bacteria, the inhibition zone diameters are 15 and 17 mm, respectively. The corresponding values for Gentamycin are 30 and 25 mm.

Table 3. Inhibition zones (mm) and MIC values (μM) against different microbes.

Tested Microbes	Inhibition Zones (mm)	MIC (μM)
A. fumigatus	14	754.6 (294) [a]
C. albicans	12	1509.3 (587) [a]
St. aureus	16	188.6 (21) [b]
B. subtilis	18	94.3 (10) [b]
E. coli	15	377.3 (10) [b]
P. vulgaris	17	377.3 (10) [b]

[a] Ketoconazole; [b] Gentamycin.

In order to further investigate the antimicrobial activity of the studied Ni(II) complex on the selected microbes, we determined the minimum inhibitory concentrations (MICs), which in turn indicate the potency of the complex to inhibit the microbial growth with a relatively low dose needed for this purpose, and the results are depicted in Table 3. The tabulated results showed that the MIC values are the lowest for the Ni(II) complex against *B. subtilis* (94.3 μM) and *S. aureus* (188.6 μM), indicating higher activities against these microbes as gram-positive bacteria than *E. coli* and *P. vulgaris* (377.3 μM for each) as gram-negative bacteria. Obviously, the MIC values of the Ni(II) complex against the studied fungi are in the range of 754.6–1509.3 μM. The results of the antimicrobial activities showed variations in activities among the pathogenic microbes and indicated that the synthesized $[Ni(MPT)(H_2O)(SCN)_2]_n$ complex has lower antimicrobial activity than ketoconazole and gentamycin as positive controls (Table 3).

2.4.2. The Cytotoxic Activity

The $[Ni(MPT)(H_2O)(SCN)_2]_n$ complex was examined for its anticancer activity using a cell viability assay against hepatocellular (HepG-2) and lung (A-549) carcinomas. The cytotoxicity results for the investigated Ni(II) complex against the tested tumor cell lines in a concentration-dependent manner are presented in Tables S1 and S2 (Supplementary Data). Also, plots for dose response curves are shown in Figure 5. The 50% inhibitory concentration (IC_{50}) is considered a measure for the inhibitory growth activity of the $[Ni(MPT)(H_2O)(SCN)_2]_n$ complex. The results of the IC_{50} values indicated moderate cell growth inhibition against HepG-2 (132.67 ± 5.14 μM) and A-549 (146.97 ± 7.34 μM) cell lines, where the $[Ni(MPT)(H_2O)(SCN)_2]_n$ complex has slightly better cytotoxic activity against the HepG-2 cell line than the A-549 lung carcinoma.

For cis-platin as a positive control and under the same experimental conditions, the IC_{50} values against the HepG-2 and A-549 cell lines were determined to be 11.92 ± 1.10 and 24.48 ± 2.03 μM, respectively. These results indicated lower cytotoxic activity for the $[Ni(MPT)(H_2O)(SCN)_2]_n$ complex compared to cis-platin. Hence, the reported data for

the Ni(II) complex indicate moderate anticancer activity against hepatocellular and lung carcinoma cell lines compared to cis-platin.

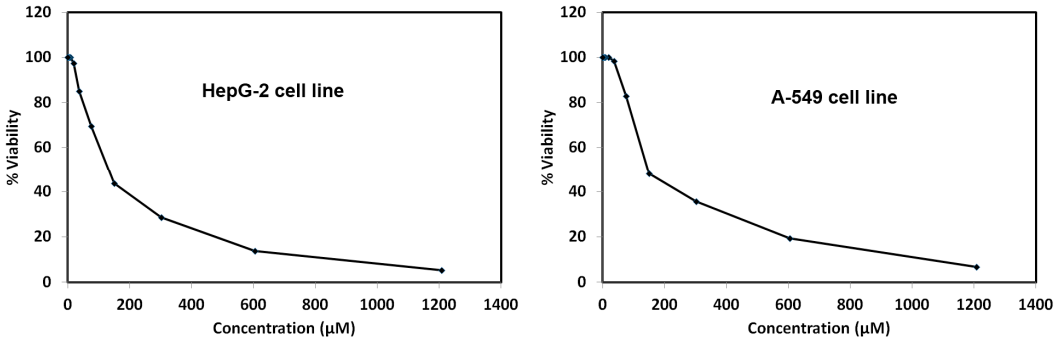

Figure 5. Cell viability assay for the cytotoxic activity of the studied Ni(II) complex against hepatocellular (HepG-2) and lung (A-549) carcinomas.

3. Materials and Methods

3.1. Synthesis of BPT Ligand

The *s*-triazine ligand (BPT) was synthesized as mentioned in Method S1 (Supporting Data) [24,25].

3.2. Synthesis of [Ni(MPT)(H_2O)($SCN)_2]_n$ Complex

The new Ni(II) complex was synthesized by mixing 10 mL of a methanolic solution of BPT (30.0 mg, 0.1 mmol) with $NiSO_4 \cdot 6H_2O$ (26.3 mg, 0.1 mmol) in 5 mL of distilled water, followed by the addition of 1 mL of saturated KSCN aqueous solution. Then, 1 mL of a 1 M H_2SO_4 solution was added to the resulting green precipitate, and the mixture was heated under reflux conditions for 2 h. The resulting green solution was filtered, and the clear filtrate was left for slow evaporation. After one week, green prismatic crystals were formed and were harvested by filtration.

Yield: $C_{11}H_{13}N_7NiO_3S_2$: (76.4%). Anal. Calc. C, 31.91; H, 3.16; N, 23.68; S, 15.49; Ni, 14.17%. Found: C, 31.68; H, 3.07; N, 23.45; S, 15.41; Ni, 14.07%. IR (KBr, cm^{-1}): 2991, 2929, 2114, 1603, 1565, 1505, 1470.

3.3. Physicochemical Characterizations

The chemicals used in the present work were purchased from their original suppliers, where all chemical details are described in the Supplementary Data. In addition, the instrument used for measuring the FTIR spectra and the machine used for single crystal X-ray measurements, as well as the information needed for solving the structure of the studied $[Ni(MPT)(H_2O)(SCN)_2]_n$ polymeric complex, were described in Supplementary Data [62–67]. The FTIR spectra of the $[Ni(MPT)(H_2O)(SCN)_2]_n$ complex and BPT ligand are shown in Figures S1 and S2 (Supplementary Data), respectively.

3.4. Biological Studies

The antibacterial activity of the $[Ni(MPT)(H_2O)(SCN)_2]_n$ complex was assessed against some selected gram-positive bacteria, namely *S. aureus*, *B. subtilis*, and gram-negative bacteria, namely *E. coli* and *P. vulgaris*, as well as the antifungal activity against the fungi, *A. fumigatus* and *C. albicans*. The minimal inhibitory concentrations (MICs) against different microbes were also determined [68]. In addition, the in vitro anticancer activities of the studied complex against hepatocellular (HepG-2) and lung (A-549) cancer cell lines were examined [69]. Further experimental details regarding the biological experiments, the cell lines, and the cytotoxicity assays were described in the supplementary data.

4. Conclusions

Heating an acidified solution of the BPT ligand with $NiSO_4 \cdot 6H_2O$ in the presence of SCN^- under reflux afforded a new 1D polymeric complex with the formula $[Ni(MPT)(H_2O)(SCN)_2]_n$. Single crystal X-ray diffraction confirmed the acid-mediated hydrolysis of the BPT ligand to 4-(3,5-dimethyl-1H-pyrazol-1-yl)-6-methoxy-1,3,5-triazin-2-ol (MPT). The latter acts as a bidentate chelate and reacts with Ni(II) in the same reaction mixture, forming the $[Ni(MPT)(H_2O)(SCN)_2]_n$ 1D polymer, in which one of the thiocyanate groups acts as a connector between the Ni(II) centers. In this complex, the Ni(II) ion is hexa-coordinated with the NiN_4SO coordination sphere, and the geometry around the metal center could be described as a slightly distorted octahedron. Evaluations of the antimicrobial and cytotoxic activities of the $[Ni(MPT)(H_2O)(SCN)_2]_n$ complex are presented. The Ni(II) complex has broad-spectrum antimicrobial activities. Also, it showed cytotoxic activity against HepG-2 and A-549 cell lines. The corresponding IC_{50} values are 132.67 ± 5.14 and 146.97 ± 7.34 μM, respectively.

Supplementary Materials: The following supporting information can be downloaded at: https://www.mdpi.com/article/10.3390/inorganics11030135/s1. Physicochemical characterizations: X-ray measurements; Method S1: Synthesis of BPT; Method S2: Biological Studies; Figure S1: FTIR spectra of the $[Ni(MPT)(H_2O)(SCN)_2]_n$ complex; Figure S2: FTIR spectra of the BPT ligand. Figure S3: ^1H and ^{13}C NMR spectra of the ligand (BPT). Chemical shifts are reported in parts per million (ppm). Table S1: The cytotoxicity of the studied complex against the HepG-2 cell line; Table S2: The cytotoxicity of the studied complex against the A-549 cell line.

Author Contributions: Conceptualization, S.M.S., A.E.-F. and R.A.M.; methodology, R.A.M., M.H. and S.M.S.; software, R.A.M., M.H. and S.M.S.; validation, R.A.M., A.E.-F., K.A.D. and S.M.S.; formal analysis, R.A.M., M.H., A.E.-F., K.A.D. and S.M.S.; investigation, R.A.M. and S.M.S.; resources, R.A.M., A.E.-F., K.A.D. and S.M.S.; data curation, R.A.M., M.H., A.E.-F. and S.M.S.; writing—original draft preparation, R.A.M., A.E.-F., M.H. and S.M.S.; writing—review and editing, R.A.M., A.E.-F., M.H., K.A.D. and S.M.S.; visualization, R.A.M. and S.M.S.; supervision, R.A.M. and S.M.S.; project administration, R.A.M., A.E.-F., K.A.D. and S.M.S.; funding acquisition, A.E.-F., K.A.D. and S.M.S. All authors have read and agreed to the published version of the manuscript.

Funding: This research received no external funding.

Data Availability Statement: Not applicable.

Conflicts of Interest: The authors declare no conflict of interest.

References

1. Orhan, N.; Uysal, S. The synthesis and characterization of s-triazine polymer complexes containing epoxy groups. *J. Mol. Struct.* **2020**, *1203*, 127370. [CrossRef]
2. Silen, J.L.; Lu, A.T.; Solas, D.W.; Gore, M.A.; Maclean, D.; Shah, N.H.; Coffin, J.M.; Bhinderwala, N.S.; Wang, Y.; Tsutsui, K.T.; et al. Screening for novel antimicrobials from encoded combinatorial libraries by using a two-dimensional agar format. *Antimicrob. Agents Chemother.* **1998**, *42*, 1447–1453. [CrossRef] [PubMed]
3. Refaat, H.M.; Alotaibi, A.A.M.; Dege, N.; El-Faham, A.; Soliman, S.M. Co(II) complexes based on the *bis*-pyrazol-s-triazine pincer ligand: Synthesis, X-ray structure studies, and cytotoxic evaluation. *Crystals* **2022**, *12*, 741. [CrossRef]
4. Foster, B.J.; Harding, B.J.; Leyland-Jones, B.; Hoth, D. Hexamethyl melamine: A critical review of an active drug. *Cancer Treat. Rev.* **1986**, *13*, 197–217. [CrossRef] [PubMed]
5. Kumar, P.V.; Tusi, S.; Tusi, Z.; Joshi, M.; Bajpai, S. Synthesis and biological activity of substituted 2,4,6-s-triazines. *Acta Pharm.* **2004**, *54*, 1–12.
6. Lasri, J.; Al-Rasheed, H.H.; El-Faham, A.; Haukka, M.; Abutaha, N.; Soliman, S.M. Synthesis, structure and in vitro anticancer activity of Pd(II) complexes of mono- and bis-pyrazolyl-s-triazine ligands. *Polyhedron* **2020**, *187*, 114665. [CrossRef]
7. Mikhaylichenko, S.N.; Patel, S.M.; Dalili, S.; Chesnyuk, A.A.; Zaplishny, V.N. Synthesis and structure of new 1, 3, 5-triazine-pyrazole derivatives. *Tetrahedron Lett.* **2009**, *50*, 2505–2508. [CrossRef]
8. Farooq, M.; Sharma, A.; Almarhoon, Z.; Al-Dhfyan, A.; El-Faham, A.; Abu Taha, N.; Wadaan, M.A.M.; de la Torre, B.G.; Albericio, F. Design and synthesis of mono-and di-pyrazolyl-s-triazine derivatives, their anticancer profile in human cancer cell lines, and in vivo toxicity in zebrafish embryos. *Bioorg. Chem.* **2019**, *87*, 457–464.
9. Horacek, H.; Pieh, S. The importance of intumescent systems for fire protection of plastic materials. *Polym. Int.* **2000**, *49*, 1106–1114. [CrossRef]

10. Gonul, I.; Ay, B.; Karaca, S.; Sahin, O.; Serin, S. Novel copper(II) complexes of two tridentate ONN type ligands: Synthesis, characterization, electrical conductivity and luminescence properties. *Inorg. Chim. Acta* **2018**, *477*, 75–83. [CrossRef]
11. Naz, A.; Arun, S.; Narvi, S.S.; Alam, M.S.; Singh, A.; Bhartiya, P.; Dutta, P.K. Cu(II)-carboxymethyl chitosan-silane Schiff base complex grafted on nano silica: Structural evolution, antibacterial performance and dye degradation ability. *Int. J. Biol. Macromol.* **2018**, *110*, 215–226. [CrossRef] [PubMed]
12. Lu, F.; Astruc, D. Nanomaterials for removal of toxic elements from water. *Coord. Chem. Rev.* **2018**, *356*, 147–164. [CrossRef]
13. Hoog, D.P.; Gamez, P.; Dressen, W.L.; Reedijk, J. New polydentate and polynucleating N-donor ligands from amines and 2,4,6-trichloro-1,3,5-triazine. *Tetrahedron Lett.* **2002**, *43*, 6783–6786. [CrossRef]
14. Mahler, J.; Rafler, G. Modified melamine resins for optical applications. *Opt. Mater.* **1999**, *12*, 363–368. [CrossRef]
15. Nuyken, O.; Scherer, C.; Baindl, A.; Brenner, A.R.; Dahn, U.; Gärtner, R.; Kaiser-Rohrich, S.; Kollefrath, R.; Matusche, P.; Voit, B. Azo-group-containing polymers for use in communications technologies. *Prog. Polym. Sci.* **1997**, *22*, 93–183. [CrossRef]
16. Yan, H.; Zhao, Z.; Ge, W.; Zhang, N.; Jin, Q. Hyperbranched polyurea as charring agent for simultaneously improving flame retardancy and mechanical properties of ammonium polyphosphate/polypropylene composites. *Ind. Eng. Chem. Res.* **2017**, *56*, 8408–8415. [CrossRef]
17. Fink, J.K. *An Overview of Methods and Standards, the Chemistry of Bio-Based Polymers*; Scrivener Publishing LLC; John Wiley & Sons, Inc.: Hoboken, NJ, USA, 2014; pp. 1–41.
18. Nedel'ko, V.V.; Shastin, A.V.; Korsunskii, B.L.; Chukanov, N.V.; Larikova, T.S.; Kazakov, A.I. Synthesis and thermal decomposition of ditetrazol-5-ylamine. *Russ. Chem. Bull.* **2005**, *54*, 1710. [CrossRef]
19. El-Faham, A.; Dahlous, K.A.; AL-Othman, Z.A.; Al-Lohedan, H.A.; El-Mahdy, G.A. Sym-trisubstituted 1,3,5-triazine derivatives as promising organic corrosion inhibitors for steel in acidic solution. *Molecules* **2016**, *21*, 436–447. [CrossRef]
20. Dahlous, K.A.; Alotaibi, A.A.M.; Dege, N.; El-Faham, A.; Soliman, S.M.; Refaat, H.M. X-ray structure analyses and biological evaluations of a new Cd (II) complex with s-triazine based ligand. *Crystals* **2022**, *12*, 861. [CrossRef]
21. Mooibroek, T.J.; Gamez, P. The s-triazine ring, a remarkable unit to generate supramolecular interactions. *Inorg. Chim. Acta* **2007**, *360*, 381–404. [CrossRef]
22. Gamez, P.; Reedijk, J. 1,3,5-triazine-based synthons in supramolecular chemistry. *Eur. J. Inorg. Chem.* **2006**, *37*, 29–42. [CrossRef]
23. Soliman, S.M.; Elsilk, S.E.; El-Faham, A. Synthesis, structure and biological activity of zinc (II) pincer complexes with 2,4-bis(3,5-dimethyl-1H-pyrazol-1-yl)-6-methoxy-1,3,5-triazine. *Inorg. Chim. Acta* **2020**, *508*, 119627. [CrossRef]
24. Soliman, S.M.; El-Faham, A. Synthesis, characterization, and structural studies of two heteroleptic Mn (II) complexes with tridentate N, N, N-pincer type ligand. *J. Coord. Chem.* **2018**, *71*, 2373–2388. [CrossRef]
25. Soliman, S.M.; El-Faham, A. One pot synthesis of two Mn (II) perchlorate complexes with *s*-triazine NNN-pincer ligand; molecular structure, Hirshfeld analysis and DFT studies. *J. Mol. Struct.* **2018**, *1164*, 344–353. [CrossRef]
26. Das, A.; Demeshko, S.; Dechert, S.; Meyer, F. A new triazine-based tricompartmental ligand for stepwise assembly of mononuclear, dinuclear, and 1D-polymeric heptacoordinate manganese(II)/azido complexes. *Eur. J. Inorg. Chem.* **2011**, *2011*, 1240–1248. [CrossRef]
27. Tilly, D.; Dayaker, G.; Bachu, P. Cobalt mediated C–H bond functionalization: Emerging tools for organic synthesis. *Catal. Sci. Technol.* **2014**, *4*, 2756–2777. [CrossRef]
28. Yoshino, T.; Matsunaga, S. Cobalt-catalyzed C(sp^3)-H functionalization reactions. *Asian J. Org. Chem.* **2018**, *7*, 1193–1205. [CrossRef]
29. Soliman, S.M.; Massoud, R.A.; Al-Rasheed, H.H.; El-Faham, A. Syntheses and structural investigations of penta-coordinated Co(II) complexes with *bis*-pyrazolo-*s*-triazine pincer ligands, and evaluation of their antimicrobial and antioxidant activities. *Molecules* **2021**, *26*, 3633. [CrossRef]
30. Refaat, H.M.; Alotaibi, A.A.M.; Dege, N.; El-Faham, A.; Soliman, S.M. Synthesis, Structure and biological evaluations of Zn(II) pincer complexes based on s-triazine type chelator. *Molecules* **2022**, *27*, 3625. [CrossRef]
31. Soliman, S.M.; El-Faham, A.; Elsilk, S.E. Novel one-dimensional polymeric Cu(II) complexes via Cu(II)-assisted hydrolysis of the 2,4-bis (3,5-dimethyl-1Hpyrazol-1-yl)-6-methoxy-1,3,5-triazine pincer ligand: Synthesis, structure, and antimicrobial activities. *Appl. Organomet. Chem.* **2020**, *34*, e5941. [CrossRef]
32. Soliman, S.M.; Al-Rasheed, H.H.; Elsilk, S.E.; El-Faham, A. A Novel centrosymmetric Fe(III) complex with anionic *bis*-pyrazolyl-*s*-triazine ligand; synthesis, structural investigations and antimicrobial evaluations. *Symmetry* **2021**, *13*, 1247. [CrossRef]
33. Lasri, J.; Haukka, M.; Al-Rasheed, H.H.; Abutaha, N.; El-Faham, A.; Soliman, S.M. Synthesis, structure and in vitro anticancer activity of Pd (II) complex of pyrazolyl-s-triazine ligand; A new example of metal-mediated hydrolysis of s-triazine pincer ligand. *Crystals* **2021**, *11*, 119. [CrossRef]
34. Soliman, S.M.; Elsilk, S.E.; El-Faham, A. Syntheses, structure, Hirshfeld analysis and antimicrobial activity of four new Co(II) complexes with s-triazine-based pincer ligand. *Inorg. Chim. Acta* **2020**, *510*, 119753.
35. Soliman, S.M.; Almarhoon, Z.; El-Faham, A. Synthesis, molecular and supramolecular structures of new Cd (II) pincer-type complexes with s-triazine core ligand. *Crystals* **2019**, *9*, 226. [CrossRef]
36. Soliman, S.M.; El-Faham, A. Synthesis, X-ray structure, and DFT studies of five and eight-coordinated Cd(II) complexes with striazine N-pincer chelate. *J. Coord. Chem.* **2019**, *72*, 1621–1636. [CrossRef]
37. Soliman, S.M.; Al-Rasheed, H.H.; El-Faham, A. Synthesis, X-ray Structure, Hirshfeld Analysis of Biologically Active Mn(II) Pincer Complexes Based on s-Triazine Ligands. *Crystals* **2020**, *10*, 931. [CrossRef]

38. Soliman, S.M.; Al-Rasheed, H.H.; Albering, J.H.; El-Faham, A. Fe(III) Complexes Based on Mono- and Bispyrazolyl-*s*-triazine Ligands: Synthesis, Molecular Structure, Hirshfeld, and Antimicrobial Evaluations. *Molecules* **2020**, *25*, 5750. [CrossRef] [PubMed]
39. Dahlous, K.A.; Soliman, S.M.; El-Faham, A.; Massoud, R.A. Synthesis, molecular and supramolecular structures of symmetric dinuclear Cd(II) azido complex with *bis*-pyrazolyl s-triazine pincer ligand. *Symmetry* **2022**, *14*, 2409. [CrossRef]
40. Dahlous, K.A.; Soliman, S.M.; El-Faham, A.; Massoud, R.A. Synthesis and X-ray structure combined with Hirshfeld and AIM studies on a new trinuclear Zn(II)-azido complex with *s*-triazine pincer ligand. *Crystals* **2022**, *12*, 1786. [CrossRef]
41. Soliman, S.M.; Almarhoon, Z.; Sholkamy, E.N.; El-Faham, A. Bis-pyrazolyl-s-triazine Ni (II) pincer complexes as selective gram-positive antibacterial agents; synthesis, structural and antimicrobial studies. *J.Mol. Struct.* **2019**, *1195*, 315–322. [CrossRef]
42. Soliman, S.M.; El-Faham, A. Synthesis, molecular structure and DFT studies of two heteroleptic nickel (II) s-triazine pincer type complexes. *J. Mol. Struct.* **2019**, *1185*, 461–468. [CrossRef]
43. Refaat, H.M.; Alotaibi, A.A.M.; Dege, N.; El-Faham, A.; Soliman, S.M. Syntheses, X-ray structure and biological studies of binuclear μ-oxo diiron complexes with s-triazine pincer ligand. *Inorg. Chim. Acta* **2022**, *543*, 121196. [CrossRef]
44. Dixon, N.E.; Gazzola, C.; Blakeley, R.L.; Zerner, B. Jack bean urease (EC 3.5.1.5). Metalloenzyme. Simple biological role for nickel. *J. Am. Chem. Soc.* **1975**, *97*, 4131–4133. [CrossRef] [PubMed]
45. Meyer, F.; Kozlowski, H. *Comprehensive Coordination Chemistry II*; McCleverty, J.A., Meyer, T.J., Eds.; Elsevier: Amsterdam, The Netherlands, 2003; Volume 6, pp. 247–554.
46. Andrews, R.K.; Blakeley, R.L.; Zerner, B. *Metal Ions in Biological Systems*; Sigel, H., Sigel, A., Eds.; Marcel Dekker Inc.: New York, NY, USA, 1988; Volume 23, pp. 165–284.
47. Kurtaran, R.; Yildirim, L.T.; Azaz, A.D.; Namli, H.; Atakol, O. Synthesis, characterization, crystal structure and biological activity of a novel heterotetranuclear complex: [NiLPb (SCN) $_2$ (DMF) (H_2O)] $_2$. *J. Inorg. Biochem.* **2005**, *99*, 1937–1944. [CrossRef]
48. Shawish, H.B.; Wong, W.; Wong, Y.; Loh, S.; Looi, C.; Hassandarvish, P.; Phan, A.; Wong, W.; Wang, H.; Paterson, I.C.; et al. Nickel(II) complex of polyhydroxybenzaldehyde N^4-thiosemicarbazone exhibits anti-inflammatory activity by inhibiting NF-κB transactivation. *PLoS ONE* **2014**, *9*, e100933. [CrossRef] [PubMed]
49. Totta, X.; Papadopoulou, A.A.; Hatzidimitriou, A.G.; Papadopoulos, A.N.; Psomas, G. Synthesis, structure and biological activity of nickel (II) complexes with mefenamato and nitrogen-donor ligands. *J. Inorg. Biochem.* **2015**, *145*, 79–93. [CrossRef] [PubMed]
50. Skyrianou, K.C.; Perdih, F.; Papadopoulos, A.N.; Turel, I.; Kessissoglou, D.P.; Psomas, G. Nickel-quinolones interaction. Part 5-Biological evaluation of nickel (II) complexes with first-, second- and third-generation quinolones. *J. Inorg. Biochem.* **2011**, *105*, 1273–1285. [CrossRef]
51. Fenger, I.; Le Drian, C. Reusable polymer-supported palladium catalysts: An alternative to tetrakis(triphenylphine) palladium in the suzuki cross-coupling reaction. *Tetrahedron Lett.* **1998**, *39*, 4287–4290. [CrossRef]
52. Elaasser, M.M.; Ibrahim, A.G.; Fahmy, A.; Osman, I.; El-Shiekh, H.H.; Abd El-Haib, F.; Salah, A.M. Synthesis, characterization and biological activity of polymer Nickel (II) complex. *J. Advan. Chem.* **2016**, *12*, 4387–4396.
53. Maspoch, D.; Ruiz-Molina, D.; Veciana, J. Magnetic nano porous coordination polymers. *J. Mater. Chem.* **2004**, *14*, 2713–2723. [CrossRef]
54. James, S.L. Metal-organic frameworks. *Chem. Soc. Rev.* **2003**, *32*, 276–288. [CrossRef] [PubMed]
55. Kaliyappan, T.; Swaminathan, C.S.; Kannan, P. Synthesis and characterization of a new metal chelating polymer and derived Ni (II) and Cu (II) polymer complexes. *Polymer* **1996**, *37*, 2865–2869. [CrossRef]
56. Zhang, X.; Fu, P.; Xiong, D.; Li, Y.; Dong, X. Synthesis, crystal structures, and magnetic properties of three nickel (II) coordination polymers based on a rigid pyrazine carboxylic acid containing different N ligands. *J. Mol. Struct.* **2022**, *1261*, 132889. [CrossRef]
57. Easson, M.; Condon, B.; Yoshioka-Tarver, M.; Childress, S.; Slopek, R.; Bland, J.; Nguyen, T.M.; Chang, S.C.; Graves, E. Cyanuric chloride derivatives for cotton textile treatment-synthesis, analysis, and flammability testing. *AATCC Rev.* **2011**, *11*, 60–66.
58. Pedersen, K.S.; Bendix, J.; Clérac, R. Single-molecule magnet engineering: Building-block approaches. *Chem. Commun.* **2014**, *50*, 4396–4415. [CrossRef] [PubMed]
59. Gatteschi, D.; Sessoli, R. Quantum tunneling of magnetization and related phenomena in molecular materials. *Angew. Chem., Int. Ed.* **2003**, *42*, 268–297. [CrossRef] [PubMed]
60. Qin, T.; Shi, Z.; Zhang, W.; Dong, X.; An, N.; Sakiyama, H.; Muddassir, M.; Srivastava, D.; Kumar, A. 2D isostructural Ln(III)-based coordination polymer derived from Imidazole carboxylic acid: Synthesis, structure and magnetic behavior. *J. Mol. Struct.* **2023**, *1282*, 135220. [CrossRef]
61. Dong, X.; Shi, Z.; Li, D.; Li, Y.; An, N.; Shang, Y.; Sakiyama, H.; Muddassir, M.; Si, C. The regulation research of topology and magnetic exchange models of CPs through Co(II) concentration adjustment. *J. Solid State Chem.* **2023**, *318*, 123713. [CrossRef]
62. Bruker, A.X.S. *APEX2—Software Suite for Crystallographic Programs*; Bruker AXS, Inc.: Madison, WI, USA, 2012.
63. Sheldrick, G.M. *SADABS—Bruker Nonius Scaling and Absorption Correction*; Bruker AXS, Inc.: Madison, WI, USA, 2012.
64. Sheldrick, G.M. SHELXT–Integrated space-group and crystal-structure determination. *Acta Cryst. A* **2015**, *71*, 3–8. [CrossRef]
65. Sheldrick, G.M. Crystal Structure Refinement with SHELXL. *Acta Crystallogr. C* **2015**, *C71*, 3–8. [CrossRef]
66. Hübschle, C.B.; Sheldrick, G.M.; Dittrich, B. ShelXle: A Qt Graphical User Interface for SHELXL. *J. Appl. Cryst.* **2011**, *44*, 1281–1284. [CrossRef] [PubMed]
67. Spek, A.L. PLATON SQUEEZE: A tool for the calculation of the disordered solvent contribution to the calculated structure factors. *Acta Cryst.* **2015**, *C71*, 9–18.

68. Mosmann, T. Rapid colorimetric assay for cellular growth and survival: Application to proliferation and cytotoxicity assays. *J. Immunol. Methods* **1983**, *65*, 55–63. [CrossRef] [PubMed]
69. Gomha, S.M.; Riyadh, S.M.; Mahmmoud, E.A.; Elaasser, M.M. Synthesis and anticancer activities of thiazoles, 1,3-thiazines, and thiazolidine using Chitosan-grafted-poly(vinylpyridine) as basic catalyst. *Heterocycles* **2015**, *91*, 1227–1243.